# Bandwidth Part and Service Differentiation in Wireless Networks

*Abstract*—**This paper presents a stochastic geometry-based model for bandwidth part (BWP) in device-to-device wireless networks. BWP allows one to adapt the bandwidth allocated to users depending on their data rate needs. Specifically, in BWP, a wide bandwidth is divided into chunks of smaller bandwidths and the number of bandwidth chunks allocated to a user depends on its needs or type. The BWP model studied here is probabilistic in that the user locations are assumed to form a realization of a Poisson point process and each user decides independently to be of a certain type with some probability. This model allows one to quantify spectrum sharing and service differentiation in this context, namely to predict what performance a user gets depending on its type and the overall performance. This is based on exact representations of key performance metrics for each user type, namely its success probability, the meta distribution of its signal-to-interference ratio, and its Shannon throughput. We also show that, surprisingly, the higher traffic variability stemming from BWP is beneficial: compare two networks using BWP and having the same mean signal and the same mean interference powers, the network with higher traffic variability performs better for all these performance metrics.**

## I. Introduction

### A. Bandwidth part (BWP) and motivation

The BWP concept is based on the division of a wide bandwidth into multiple smaller chunks of bandwidth. The main aim of this division is to let the number of bandwidth chunks used by a wireless user depend on its type at a given time, namely on its current needs in terms of data rate or constraints in terms of power consumption. This new flexibility on what is allocated to users makes of BWP a new and quite fascinating dimension of radio spectrum sharing.

The flexibility due to BWP is particularly important in future wireless networks, *e.g.*, 5G networks, which need to accommodate a larger variety of wireless devices (see Table I), running in turn a larger variety of wireless applications with highly heterogeneous throughput demands (see Table I). More specifically, as shown in Table I, mobile video streaming constitutes the majority of wireless traffic and requires higher data rate and hence wider spectrum allocation in the BWP setting. In contrast, text or e-mail applications have lower data rate requirements and would thus be allocated less bandwidth. For users of the latter type, the use of wide bandwidth leads to high idling power consumption by radio-frequency (RF) and baseband signal processing circuitry. Hence, the use of different bandwidth sizes allows a balance between the data rate variations and power consumed by the users.

One typical use case is that of web browsing, where the user is active for a short time on wide bandwidth to accommodate the bursty traffic (download of a web page with pictures), and then stays active on narrow bandwidth for the time until it again encounters bursty traffic situation.

TABLE I
Types of wireless devices, wireless applications, and heterogeneous throughput demands. The numbers in parentheses refer to 2017 and 2022, respectively. (Sources: Cisco VNI Mobile, 2019 [1] and MediaTek white paper [2].)

| | Wireless devices [1] | | Wireless applications [2] | |
|---|---|---|---|---|
| | % Share (2017, 2022) | % Growth (2017, 2022) | Throughput demand (Mbps) | |
| Smartphones + phablets | (50, 44) | (88, 93) | Streaming video | Video (1.5) |
| | | | | HD video (5) |
| M2M | (11, 31) | (1.8, 2.2) | Online gaming | Min (1) |
| | | | | Full (25) |
| Nonsmartphones | (34, 10) | (1.3, 0.3) | Video service & sharing | Min (0.5) |
| | | | | HD video (2) |
| | | | | HD video sharing (10) |
| Tablets | (2, 3) | (4.6, 2.9) | VoIP | Voice (0.1) |
| | | | | HD video (1.5) |
| PCs | (2, 1) | (4.3, 1.6) | Social media | Text (0.3) |

Due to this power-saving feature of BWP, the 3rd Generation Partnership Project (3GPP) has recently proposed to include BWP in 5G New Radio (NR) and to make NR wide bandwidth operations energy efficient [3, Section 6.10], [4, Section 4.4.5].

The benefits of the flexibility offered by BWP are hence multiple. Not only this adaptation saves energy for those applications and devices with lower data rate requirement or bursty traffic, but this in turn diminishes the interference incurred by other nearby devices of all types. Indeed, due to the broadcast nature of the wireless medium, users interact with each other through mutual interference. The higher the bandwidth, the higher the interference.

Hence the bandwidth adaption of BWP has two competing effects. On the positive side, a higher bandwidth increases the signal power and hence the throughput of a given application. On the negative side, it increases the interference power, which has a detrimental collective effect. As a result, it is fair to say that there is no global understanding of the effect of BWP on bandwidth sharing.

As of now, to the best of our knowledge, the BWP proposal for 5G NR is still in a development phase, and there is no concrete model available for BWP. Also, most of existing studies on BWP (discussed in Section I-C) are restricted to the investigation of power savings. The study of the key wireless network performance metrics is an open area. In particular, there is currently no known way to predict the effect of the

BWP adaptation on the performance of a user of a given type.

The main motivation of the present paper can now be stated in simple terms: it is to provide a statistical model allowing one to analyze the bandwidth sharing provided by BWP in device-to-device (D2D) wireless networks, and more precisely to predict the key performance metrics of the typical user of a given type in this context. It is appropriate to stress the analogy with the theory of differentiated services in wireline networks (DiffServ [5]), which was instrumental in classifying and managing different types (classes) of network traffic and in predicting their interactions. The aim of this paper is to make a first step in the direction of a quantitative theory for BWP bandwidth sharing and the management of different types of network traffic in this class of wireless networks.

### B. Contributions

**A BWP model.** The first contribution of this paper is a stochastic model for BWP in infrastructureless wireless networks, where the type of the user is determined by the number of bandwidth chunks it uses. The model supports service differentiation in wireless networks by capturing interaction among different types of wireless users. Specifically, the BWP model allows one to calculate the performance achieved by each type of user.

**Performance analysis.** Using tools from stochastic geometry for D2D networks, we provide expressions for key wireless network performance metrics, namely, success probability, meta distribution of the signal-to-interference ratio (SIR), Shannon throughput, and Shannon throughput per Joule. These expressions permit the evaluation of per-type and overall performance metrics.

**Different performance viewpoints.** Using the per-type and the overall performance, the BWP model allows one to analyze the bandwidth sharing from the viewpoints of both users and operators. Per-type performance is more important for users, while overall performance might be important too from the operator's viewpoint due the link between this and pricing. Thus, the machinery proposed here to predict both should be useful to help an operator make a choice between the following options: 1) allocate the entire bandwidth (*i.e.*, implement no BWP), 2) adaptively allocate bandwidth chunks (*i.e.*, implement BWP).

**The mean model.** BWP introduces additional randomness due to the probabilistic selection of the set of bandwidth chunks depending on the user type. We show that the increased variability in traffic due to BWP may improve the performance for the same mean interference and the same mean signal powers. This is particularly useful when comparing two networks based on BWP but with different mix of user types.

### C. Related work

Traffic profiling in wireline networks has been a key objective to monitor, manage, and optimize the network. Traffic-flow characterization has received significant attention for networks consisting of users running different types of applications. To understand the behavior of heterogeneous flows and their interactions, flows have been classified based on their features, for example: traffic size (as *elephant* and *mouse*) [6]–[8], time duration (as *tortoise* and *dragonfly*) [9], rate (as *cheetah* and *snail*) [10], and burstiness (as *porcupine* and *stingray*) [10]. For wireless networks as well, in the BWP setting, one can make an analogy to elephants and mice: users needing wide bandwidth (large number of bandwidth chunks) can be viewed as *elephants*, while users needing small bandwidth (small number of bandwidth chunks) as *mice*.

As alluded to earlier, the 3GPP has very recently considered the inclusion of BWP in 5G NR to enable spectrum flexibility and power savings [3, Section 6.10], [4, Section 4.4.5]. The literature on how BWP affects power savings, throughput, and reliability is very limited. For instance, [11] discusses power savings due to BWP. Since a user need not transmit or receive outside the bandwidth allocated to it, the user consumes less power in some scenarios, for example, involving bursty traffic. The work in [12] studies the effect of BWP on reliability and fairness in wireless networks. But these works on BWP use simulations as a tool to evaluate the performance based on the few (still developing) guidelines from the 3GPP about BWP.

This paper is focused on BWP for D2D networks. There exists a large number of works on spectrum allocation including multi-channel scenarios in standalone D2D networks or D2D networks sharing spectrum with cellular networks. For instance, see [13]–[15] and references therein. In relation to heterogeneity among devices in a D2D network based on allocated bandwidth, [16] focuses on the dynamic allocation of bandwidth to unlicensed users based on data rate demand provided the allocated spectrum is unoccupied by licensed users and other unlicensed users. This results in an orthogonal bandwidth allocation to avoid mutual interference. Using a simulation approach, the work in [17] takes battery life into account and tries to maximize the number of completed transmissions as a function of already allocated bandwidth.

Stochastic geometry, which is the main tool used in the present paper, has been extensively used to model and analyze both infrastructureless (*e.g.*, D2D) and infrastructure (*e.g.*, cellular) networks [18]–[21]. Especially, Poisson point process (PPP)-based models have been very popular for the analysis of wireless networks. Heterogeneous PPP based cellular networks were in particular discussed in [22]. These models feature several types of base stations and a single class of users associating e.g. to the closest base station. In contrast, the setting discussed here features different types of transmitters with dedicated receivers and adapting their bandwidths to their needs.

In [23] the authors aim to maximize the density of successful transmissions given an outage constraint at the typical user. The user always selects one bandwidth chunk uniformly at random irrespective of its need. For the same bandwidth partitioning scheme as [23], [24] analyzes the mean local delay, which is the average number of transmission slots until a successful transmission. As in [23], the work in [25] maximizes the density of successful transmissions, but for frequency-selective channels, where again only one bandwidth chunk is selected for the transmission. To the best of our knowledge, no concrete BWP models accommodating different types of users are available in the literature.

## II. System Model

### A. Network model

We consider infrastructureless wireless networks such as ad hoc, D2D, and machine-to-machine (M2M) networks.[1] The transmitters are randomly located according to a homogeneous Poisson point process (PPP) $\Phi \subset \mathbb{R}^2$ of intensity $\lambda$. Each transmitter has a receiver at fixed distance $R$ in a random direction.[2] This model is also known as the *Poisson bipolar network* since the transmitter-receiver pairs can be viewed as bipoles [18]. Since the homogeneous PPP is stationary, one can just focus on the reference link between a receiver at the origin $o$ and its associated transmitter at $x_0 \in \Phi$ with $\|x_0\| = R$. Averaging over $\Phi$, this representative link becomes the *typical* link in that it has the same statistical properties as those obtained by averaging over all other links in the network.

A transmission is subject to some path loss, where the path-loss function is given by $\ell(r)$ for distance $r$. Furthermore, the transmissions experience Rayleigh fading, where the channel power gain is an exponential random variable with mean 1. Let $h_x$ denote the channel power gain between the typical receiver at the origin and the transmitter at $x \in \Phi$ due to fading. Then $h_x \sim \exp(1)$. We focus on the interference-limited scenario, where the noise power is negligible compared to the interference power.

### B. Bandwidth part model

Let $W$ be the total bandwidth available to users. Without loss of generality, we assume $W = 1$. Our bandwidth part model is as follows:

(1) The total bandwidth is divided into $K$ orthogonal chunks of equal bandwidth of $1/K$.

(2) Depending on how many chunks a transmitter uses, the transmitters are categorized into $K$ types. A type-$i$ transmitter selects $i$ $(1 \leq i \leq K)$ chunks for its transmission. In other words, the type of the user is decided by the amount of bandwidth used by that user. Let $\mathcal{T} = \{\mathcal{T}_1, \mathcal{T}_2, \ldots, \mathcal{T}_K\}$, where $\mathcal{T}_i$ is the set of all subsets $\mathcal{T}_{i,q}$ of $[K] \triangleq \{1, 2, \ldots, K\}$ of cardinality $i$, *i.e.*, $|\mathcal{T}_{i,q}| = i$ with $q = 1, 2, \ldots, \binom{K}{i}$. Here, $\binom{K}{i}$ is the number of possible ways of selecting $i$ chunks from $K$ chunks, *i.e.*, $|T_i| = \binom{K}{i}$. For example, for $K = 3$, a type-2 transmitter, *i.e.*, $i = 2$, can select two from three chunks 1, 2, and 3, *i.e.*, we have $\mathcal{T}_2 = \{\{1,2\}, \{2,3\}, \{1,3\}\}$.

(3) A type-$i$ transmitter further selects a set of chunks from $\mathcal{T}_i$ uniformly at random. For the aforementioned example with $K = 3$, a type-2 transmitter selects 2 chunks for transmission, and it does so by selecting one of the possible sets of chunks from $\{1,2\}, \{2,3\}$, and $\{1,3\}$ at random.

(4) Each transmitter independently decides to be of $i$th type with probability $p_i$ with $\sum_{i=1}^{K} p_i = 1$.

The probabilities $p_i$ quantify service differentiation. Specifically, these probabilities can be obtained from the statistical analysis of the user traffic. For instance, $p_i$ could be set according to what proportion of user's data traffic consists of large data transfer such as video streaming and what proportion consists of small traffic such as text or e-mail transmissions. As Table I in Section I-A shows, a user's traffic consists of traffic from different wireless applications with heterogeneous throughput demands. Thus, the probabilities $p_i$ could be set according to the user's throughput demands. Let us consider a use case: [1] reports that, in 2018 approximately 63% of the traffic of a mobile user was video content, and it will grow to 79% in 2022. Due to higher throughput demand for video, a mobile user is likely to request a wider bandwidth (and hence a large number of bandwidth chunks).

### C. Signal-to-interference ratio (SIR)

In interference-limited wireless networks, many key performance metrics are based on SIR. The SIR at the typical receiver located at the origin $o$ with respect to its associated transmitter at $x_0 \in \Phi$ is given by $\mathsf{SIR}_o \triangleq \frac{S}{I}$, where $S$ and $I$ are the received signal power and the interference power at the origin, respectively.

In BWP, the received SIR depends on the type of the typical user because the signal and interference powers are functions of the bandwidth allocated to the user. Without loss of generality, we condition on the fact that the typical transmitter is of type $k$, *i.e.*, it uses $1 \leq k \leq K$ chunks for transmission.

**Signal power**: We assume that a transmitter spends power $P$ per chunk used for a transmission.[3] Hence, $P$ is expressed in Joule-s$^{-1}$-Hz$^{-1}$. The received signal power at the typical receiver is given by $S_k = kPh_{x_0}\ell(x_0)$, since the typical transmitter selects $k$ chunks for transmission. Here, $h_{x_0} \sim \exp(1)$ denotes the channel power gain on the typical link.

**Interference power**: The interference caused by an interferer to the typical receiver depends on the number of overlapping chunks between that interfering transmitter and the typical transmitter. Let $t_x^{(k)}$ denote the number of such overlapping chunks between an interferer at $x \in \Phi$ and the typical transmitter (of type $k$). Then, the interference power at the typical receiver is given by

$$I_k = \sum_{x \in \Phi \setminus \{x_0\}} P t_x^{(k)} h_x \ell(x). \tag{1}$$

A type-$i$ interfering transmitter selects $i$ chunks with probability $p_i$ independent of other transmitters. Hence, the original PPP $\Phi \setminus \{x_0\}$ of interferers can be split into $K$ independent PPPs of intensities $\lambda p_i$, $i = 1, 2, \ldots, K$. Let $\Phi_i \setminus \{x_0\}$ denote the PPP of type-$i$ interferers. Let the typical transmitter select a set of $k$ chunks as $T_{k,u}$ with $1 \leq u \leq \binom{K}{k}$.

[1] As shown in Table I, in year 2022, 31% of mobile devices are expected to belong to M2M networks.

[2] Our results can also be extended to the case of random link distances.

[3] This assumption is in line with the proposed BWP model for 5G, where the transmit power is mentioned in terms of the power spectral density.

Also suppose a type-$i$ interferer selects a set of $i$ chunks as $T_{i,v}$ with $1 \le v \le \binom{K}{i}$. Then the interference power from the transmitter at $x \in \Phi \setminus \{x_0\}$ to the typical receiver is $P|T_{k,u} \cap T_{i,v}|h_x\ell(x)$, where $|T_{k,u} \cap T_{i,v}|$ is the number of overlapping chunks between a type-$i$ interferer and the typical transmitter. Let $0 \le t \le k \wedge i \le K$ denote the number of overlapping chunks between a type-$i$ interfering transmitter and the typical transmitter, where $k \wedge i$ means $\min(k, i)$. Note that $t$ is a random variable since the typical and interfering transmitters select $k$ and $i$ chunks, respectively, uniformly at random. For notation simplicity, we do not always indicate the dependence of $t$ on $k$ and $i$.

Depending on the number of overlapping chunks $t$, the PPP $\Phi_i$ can further be partitioned into $t$ independent PPPs denoted by $\Phi_{i,t}$. The PPP $\Phi_{i,t}$ corresponds to transmitters located at $x \in \Phi_i$ that have $0 \le t \le k \wedge i$ chunks common with the typical transmitter. Consequently, the interference power received at the typical receiver at the origin from type-$i$ interferers is given by

$$I_{k,i} = \sum_{t=0}^{k\wedge i} \sum_{x\in\Phi_{i,t}\setminus\{x_0\}} tPh_x\ell(x). \tag{2}$$

The total interference power at the typical receiver of type $k$ follows as

$$I_k = \sum_{i=1}^{K} I_{k,i}. \tag{3}$$

**SIR expression**: Following the expressions of signal and interference powers, the SIR experienced at the typical link of type $k$ can be expressed as

$$\mathsf{SIR}_o^{(k)} = \frac{kh_{x_0}\ell(x_0)}{\sum_{i=1}^{K}\sum_{t=0}^{k\wedge i}\sum_{x\in\Phi_{i,t}\setminus\{x_0\}} th_x\ell(x)}. \tag{4}$$

Note that the transmit power per chunk $P$ vanishes from the SIR expression.

## III. Performance Metrics

In this section, we define and discuss the three performance metrics that we consider in this work. These metrics are based on the SIR received at the typical receiver and shed light on different aspects of the performance of users.

Although the definitions of the performance metrics are general, the calculation of these metrics depends on the type of the typical user. The overall performance can be evaluated by unconditioning with respect to the type of the typical transmitter. For instance, let $f_k$ be some performance function conditioning on the fact that the typical transmitter is of type $k$. Then, the overall performance $f$ of the typical user is given by $f = \sum_{k=1}^{K} p_k f_k$. For the notation simplicity, in this section, we do not explicitly show the dependence of the performance metrics on $k$ while defining them. However, we shall reintroduce the parameter '$k$' in the performance analysis done in Section IV.

### A. Success probability

**Definition 1** (Success probability)**.** *The success probability of the typical user at the origin $o$ is the complementary cumulative distribution function (ccdf) of the SIR, which is*

$$p_{\mathrm{s}}(\theta) \triangleq \mathbb{P}_o^!(\mathsf{SIR}_o > \theta), \tag{5}$$

*where $\theta \in \mathbb{R}^+$ is the target SIR threshold.*

Here, $\mathbb{P}_o^!(\cdot)$ denotes the reduced Palm probability of the receiver point process. $p_{\mathrm{s}}$ is an outage-based performance metric: if the received SIR at the typical receiver is larger than $\theta$, the transmission is considered successful. The probability $1 - p_{\mathrm{s}}$ is known as the outage probability.

When the underlying point process is ergodic, $p_{\mathrm{s}}$ can also be interpreted as the fraction of concurrent transmissions that achieve an SIR greater than $\theta$ in each realization of the network. In other words, $p_{\mathrm{s}}$ is nothing but a *spatial average* in that it is evaluated by taking a certain expectation over the point process. This average is certainly very useful in wireless networks, but it does not provide information about individual user (link) success probabilities. Hence, to analyze the fine-grained performance, we need to quantify how individual link success probabilities are distributed around the average $p_{\mathrm{s}}$. The meta distribution of the SIR defined below is one such fine-grained performance metric in wireless networks [26].

### B. Meta distribution of the SIR

We are interested in the random variable $P_{\mathrm{s}}$ defined as

$$P_{\mathrm{s}}(\theta, \Phi) \triangleq \mathbb{P}(\mathsf{SIR} > \theta \mid \Phi), \tag{6}$$

where the conditional probability is taken over the fading and the random channel access scheme of interferers determined by the BWP model. This conditional random variable is the probability that the fading and the random channel access scheme yielding an SIR at least $\theta$ for the link (user) under consideration for a given realization of the point process $\Phi$. Hence, $P_{\mathrm{s}}$ is the success probability of that link (user) conditioned on the point process $\Phi$. The distribution of $P_{\mathrm{s}}$ obtained by taking an expectation over the point process is the meta distribution of the SIR. Formally, it is defined as follows.

**Definition 2** (Meta distribution)**.** *The meta distribution of the SIR is the distribution function*

$$\bar{F}(\theta, x) \triangleq \mathbb{P}_o^!(P_{\mathrm{s}}(\theta, \Phi) > x), \quad \theta \in \mathbb{R}^+, x \in [0, 1]. \tag{7}$$

Since $\bar{F}(\theta, x)$ is the distribution of the (conditional) distribution of the SIR, it is called the meta distribution of the SIR.

The meta distribution $\bar{F}(\theta, x)$ is the probability that the link (user) under consideration has a reliability at least $x$ for the target SIR threshold of $\theta$, where the reliability is the conditional success probability $P_{\mathrm{s}}(\theta, \Phi)$. When the underlying point process is ergodic (such as the PPP), $\bar{F}(\theta, x)$ can be interpreted as the fraction of users that achieve the target SIR of $\theta$ with probability at least $x$. The parameter $x$ can be viewed as the target reliability.

**Connection of $\bar{F}(\theta, x)$ to $p_{\rm s}(\theta)$**: The standard success probability $p_{\rm s}(\theta)$ given in (5) is the mean of the conditional random variable $P_{\rm s}(\theta, \Phi)$. Hence, the meta distribution of the SIR $\bar{F}(\theta, x)$ provides much sharper SIR performance compared to its mean $p_{\rm s}(\theta)$.

### C. Shannon throughput

The success probability $p_{\rm s}(\theta)$ and the meta distribution $\bar{F}(\theta, x)$ correspond to the binary event whether the SIR is larger than some threshold $\theta$ or not. Hence, they fail to use the SIR values larger than $\theta$ and reduce the SIR threshold $\theta$ to avoid outages if the SIR value is smaller than $\theta$. Instead, a transmitter can (if possible) adapt to channel conditions and adjust the SIR threshold $\theta$ to the maximum value such that $\mathsf{SIR} \geq \theta$ (alternatively, adapt the coding rate). In this case, Shannon throughput is a more suitable performance metric to quantify the performance in wireless networks.

**Definition 3** (Shannon throughput)**.** *Let $B$ be the bandwidth used for the transmission on a link. Shannon throughput over that link is*

$$\mathcal{R} \triangleq B\mathbb{E}(\log_2(1 + \mathsf{SIR})). \tag{8}$$

Shannon throughput is the average of the instantaneous throughput $B \log_2(1 + \mathsf{SIR})$ of a random user in the network with adaptive coding, where the SIR corresponds to that random user. Shannon throughput is expressed in bits/s.

## IV. Performance Analysis

In this section, we calculate the expressions of the performance metrics. We also analyze the allocation of contiguous bandwidth chunks in the BWP setting suggested by the 3GPP for 5G NR.

### A. Success probability

We obtain a closed-form expression of the success probability. Although our analysis can be generalized to arbitrary path loss models, we first focus on the standard power-law path loss function given as $\ell(x) = \|x\|^{-\alpha}$ with $\alpha > 2$ being the path loss exponent. We later provide a simple closed-form expression of the success probability for the bounded path loss function $\ell(x) = (c_0 + \|x\|^{\alpha})^{-1}$ with $c_0 > 0$.

**Lemma 1.** *Conditioned on the typical transmitter being of type $k$, i.e., when $x_0 \in \Phi_k$, the success probability $p_{\rm s}^{(k)}$ of the typical receiver at the origin can be expressed as*

$$p_{\rm s}^{(k)}(\theta) = \prod_{i=1}^{K} p_{\rm s}^{(k,i)}(\theta), \tag{9}$$

*where $p_{\rm s}^{(k,i)}$ is the success probability of the typical receiver due to the interference from type-$i$ interferers only conditioned on the typical transmitter being of type $k$.*

*Proof:* See Appendix A. ■

The probabilities $p_{\rm s}^{(k,i)}$ quantify the performance of differentiated services. Specifically, as shown in the following theorem, by just playing with the values of $k$ and $i$, one can investigate how elephants (users with wider bandwidth) affect the performance of mice (users with smaller bandwidth) and vice-versa. The following theorem gives a simple closed-form expression of $p_{\rm s}^{(k,i)}$ that allows one to quantify the effect of type-$i$ users on the success probability of a type-$k$ user.

**Theorem 1.** *Let us condition on the typical transmitter being type-$k$ user. For the power-law path loss model, the success probability $p_{\rm s}^{(k,i)}$ of the typical user is*

$$p_{\rm s}^{(k,i)}(\theta) = \exp\left(-\lambda p_i C \theta^{\delta} \sum_{t=0}^{k \wedge i} p_{k,i}^{(t)} \left(\frac{t}{k}\right)^{\delta}\right), \tag{10}$$

*where $C \triangleq \pi R^2 \Gamma(1+\delta)\Gamma(1-\delta)$ with $\delta \triangleq 2/\alpha$ and*

$$p_{k,i}^{(t)} = \frac{\binom{k}{t}\binom{K-k}{i-t}}{\binom{K}{i}} \tag{11}$$

*is the probability that an interferer of type $i$ has $t$ chunks common with the typical transmitter, conditioned on the fact that the latter is a type-$k$ user.*

*Proof:* See Appendix B. ■

Finally, unconditioning on the type of the typical transmitter yields the overall success probability $p_{\rm s}$ as

$$\begin{aligned} p_{\rm s}(\theta) &= \sum_{k=1}^{K} p_k p_{\rm s}^{(k)}(\theta) \\ &= \sum_{k=1}^{K} p_k \exp\left(-\lambda C \theta^{\delta} \sum_{i=1}^{K} p_i \sum_{t=0}^{k\wedge i} p_{k,i}^{(t)} \left(\frac{t}{k}\right)^{\delta}\right). \end{aligned} \tag{12}$$

**Bounded path loss function**: For the bounded path loss function $\ell(x) = (c_0 + \|x\|^{\alpha})^{-1}$ with $c_0 > 0$, we have

$$p_{\rm s}^{(k,i)}(\theta) = \exp\left(-\lambda p_i C_b \theta \sum_{t=0}^{k\wedge i} p_{k,i}^{(t)} \left(\frac{t}{k}\right)\left(\frac{\theta t}{k}(c_0 + R^{\alpha}) + c_0\right)^{\delta-1}\right), \tag{13}$$

where $C_b \triangleq \pi(c_0 + R^{\alpha})\Gamma(1+\delta)\Gamma(1-\delta)$. The proof follows the one of Theorem 1. The standard path loss function $\ell(x) = \|x\|^{-\alpha}$ is a special case of the bounded path loss function $(c_0 + \|x\|^{\alpha})^{-1}$ with $c_0 = 0$. The equations (9) and (12) are also valid for the bounded path loss case.

### B. Meta distribution of the SIR

The brief idea to evaluate the meta distribution of the SIR $\bar{F}(\theta, x)$ is to first condition on the point process $\Phi$ and then calculate the conditional random variable $P_{\rm s}$ defined in (6) by averaging over the fading and the random channel access scheme of interferers determined by the BWP model. The next step is to calculate the ccdf in (7). However, the direct calculation of the ccdf is impossible. Hence we take an indirect route, where we first calculate $b$th moments ($b \in \mathbb{C}$) of $P_{\rm s}$ and use those moments to obtain the ccdf $\bar{F}(\theta, x)$ accurately using the Gil-Pelaez theorem [27] or approximately by matching the first and second moments to those of the beta distribution [26]. In other words, averaging over the point process $\Phi$ and averaging over the fading and the random channel access scheme are done separately. This is unlike the calculation of the success probability $p_{\rm s}$, where averaging over $\Phi$, the fading, and the random channel access scheme are done simultaneously.

**Theorem 2.** *Conditioning on the typical transmitter being of type $k$, the $b$-th moment of $P_{\rm s}^{(k)}$ is*

$$M_b^{(k)} = \exp\left(-2\pi\lambda\int_0^\infty\left[1-\left(\sum_{i=1}^{K}p_i\sum_{t=0}^{k\wedge i}\frac{p_{k,i}^{(t)}}{1+\theta\frac{t}{k}\frac{\ell(r)}{\ell(x_0)}}\right)^b\right]{\rm d}r\right),$$

*where $p_{k,i}^{(t)}$ is given by* (11).

*Proof:* See Appendix C. ∎

### C. Shannon throughput

**Theorem 3.** *Conditioning on the typical transmitter being of type $k$, Shannon throughput $\mathcal{R}^{(k)}$ is given by*

$$\mathcal{R}^{(k)} = \frac{k}{K}\int_0^\infty p_{\rm s}^{(k)}(2^y-1)\ {\rm d}y, \tag{14}$$

*where $p_{\rm s}^{(k)}$ is given by* (9).

*Proof:* A transmitter of type $k$ has $k/K$ Hz of bandwidth for the transmission. Hence, we have

$$\begin{aligned}\mathcal{R}^{(k)} &= \frac{k}{K}\int_0^\infty \mathbb{P}(\log_2(1+\mathsf{SIR}_o) > y \mid x_0\in\Phi_k)\ {\rm d}y\\ &= \frac{k}{K}\int_0^\infty p_{\rm s}^{(k)}(2^y-1)\ {\rm d}y. \end{aligned} \tag{15}$$

∎

Overall Shannon throughput of the typical user follows as $\mathcal{R}=\sum_{k=1}^{K}p_k\mathcal{R}^{(k)}$.

**Shannon throughput per Joule**: In 5G NR, a key motivation for proposing the inclusion of BWP is to allow for flexible bandwidth use to reduce the power expenditure. Hence, we consider Shannon throughput per Joule of the energy spent, which is the Shannon throughput divided by the spent power $kP$. Conditioning on the typical transmitter being of type $k$, Shannon throughput per Joule $\mathcal{R}_J^{(k)}$ is obtained by dividing (15) by $kP$ as

$$\mathcal{R}_J^{(k)} = \frac{1}{KP}\int_0^\infty p_{\rm s}^{(k)}(2^y-1)\ {\rm d}y. \tag{16}$$

Here, Shannon throughput is expressed in bits/Joule.

### D. The case of contiguous bandwidth chunks

The current 5G NR guideline about BWP suggests the use of contiguous bandwidth chunks, which can easily be integrated in our BWP model. In fact, this case of contiguous bandwidth chunks is a variant of the proposed BWP model because the set of contiguous chunks is a subset of $\mathcal{T}_i$ defined in Section II-B. For a type-$i$ user, there are $K-i+1$ sets of contiguous chunks. A natural way for type-$i$ user to select one of $K-i+1$ sets of contiguous chunks is to do so uniformly at random.

That said, the performance analysis for the contiguous case is almost the same except for the expression of the probability $p_{k,i}^{(t)}$ that an interferer of type $i$ has $t$ chunks common with the typical transmitter conditioned on that the latter is a type-$k$ user. For the contiguous bandwidth chunks case, $p_{k,i}^{(t)}$ can be expressed as

$$p_{k,i}^{(t)} = \frac{2(K+t-k-i+1)}{(K-k+1)(K-i+1)}.$$

The rest of the formulas remain the same.

## V. The Mean Model

Suppose the network operator has decided to use BWP. There are several BWP configurations to choose from based on the values of the probabilities $p_k$. From the operator's viewpoint, it is natural to investigate how two networks with different $p_k$ fare in terms on the overall performance. To fairly compare two BWP-based networks, it is natural to do so for the same mean signal and the same mean interference powers.

**Mean signal power**: For the BWP model, since the typical transmitter is of type $k$ with probability $p_k$, the mean signal power at the typical receiver is given by

$$\bar{S}_k = P\ell(x_0)\sum_{k=1}^{K}p_k k. \tag{17}$$

For another network with different $p_k$, say $p_k'$, we might have to adjust the transmit power per chunk $P'$ to have the mean signal power $\bar{S}_k'$ same as $\bar{S}_k$. From (17), it follows that

$$P' = \frac{P\sum_{k=1}^{K}kp_k}{\sum_{k=1}^{K}kp_k'} \tag{18}$$

leads to $\bar{S}_k=\bar{S}_k'$.

**Mean interference power**: For the BWP model, conditioned on the fact that the typical link is of type $k$, the mean interference power is obtained by taking the expectation of $I_k$ given in (1) as

$$\begin{aligned}\mathbb{E}[I_k] &= \sum_{i=1}^{K}\sum_{t=0}^{k\wedge i}\mathbb{E}\left[\sum_{x\in\Phi_{i,t}\setminus\{x_0\}}tP\ell(x)\right]\\ &\overset{(a)}{=} \lambda\pi\delta c_0^{\delta-1}\Gamma(\delta)\Gamma(1-\delta)P\sum_{i=1}^{K}p_i\sum_{t=0}^{k\wedge i}tp_{k,i}^{(t)}, \end{aligned} \tag{19}$$

where $(a)$ is obtained by the straightforward application of the Campbell's theorem for the PPP $\Phi_{i,t}$ [18] and using the bounded path loss function $\ell(x)=(c_0+\|x\|^\alpha)^{-1}$ with $\delta\triangleq 2/\alpha$.[4] Unconditioning on the type of the typical link yields the mean interference power at the typical receiver as

$$\bar{I} = \sum_{k=1}^{K}p_k\mathbb{E}[I_k]. \tag{20}$$

For another BWP-based network with probabilities $p_k'$, the mean interference power $\bar{I}'$ can be calculated by replacing $p_k$ by $p_k'$ and $\lambda$ by $\lambda'$ in (19) and (20), where $\lambda'$ is the intensity of the PPP corresponding to the network with $p_k'$. The intensity $\lambda'$ is chosen such that the mean interference powers for two

[4]The standard path loss function $\ell(x)=\|x\|^{-\alpha}$ follows from the bounded path loss function as $c_0\to 0$.

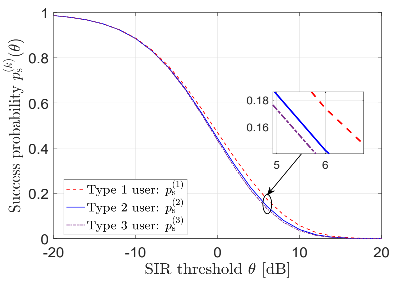


Fig. 1. Per-type success probability $p_{\mathrm{s}}^{(k)}$ versus the SIR threshold $\theta$. $p_k = 1/K = 1/3$.

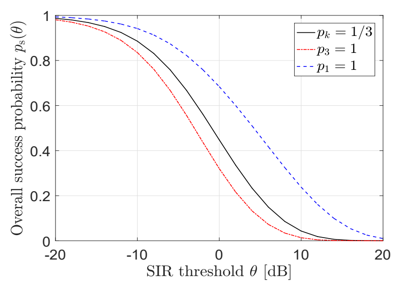


Fig. 2. Overall success probability $p_{\mathrm{s}}$ versus the SIR threshold $\theta$.

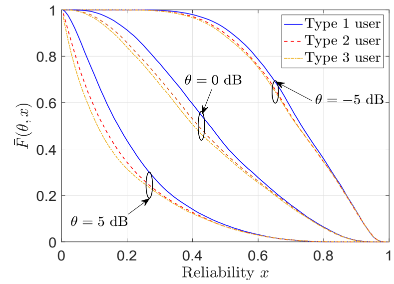


Fig. 3. The SIR meta distribution $\bar{F}(\theta, x)$ versus the reliability threshold $x$. $p_k = 1/K = 1/3$.

networks with $p_k$ and $p'_k$ are the same, *i.e.*, $\bar{I} = \bar{I}'$. Hence, from (19) and (20), it follows that

$$\lambda' = \frac{\lambda P \sum_{k=1}^{K} p_k \sum_{i=1}^{K} p_i \sum_{t=0}^{k \wedge i} t p_{k,i}^{(t)}}{P' \sum_{k=1}^{K} p'_k \sum_{i=1}^{K} p'_i \sum_{t=0}^{k \wedge i} t p_{k,i}^{(t)}}, \tag{21}$$

which results in $\bar{I} = \bar{I}_K$.

## VI. Results and Discussions

In this section, we discuss the results for the BWP model. We divide this section in two parts. The first part provides results that focus on the per-type and the overall performance in the BWP setting. The second part integrates the mean model discussed in Section V.

Without loss of generality, we assume the following model parameters. The number of bandwidth chunks is $K = 3$. The intensity of the PPP is $\lambda = 0.2$. For the bounded path loss model, the path loss exponent is $\alpha = 4$ with $c_0 = 1$. The desired link distance is $R = 1$. Other parameters are given in the captions of the relevant figures.

### A. Per-type and overall performance

**Success probability:** Figure 1 illustrates the per-type success probability given by (9). A type-1 user experiences a smaller interference compared to type-2 and type-3 users since it experiences interference only on one chunk selected randomly. Hence, a type-1 user achieves the highest success probability. As a consequence of this result on the per-type success probability, when we uncondition on the type of the user and calculate the overall success probability, the network model where a user always selects only one chunk at random (the model with $p_1 = 1$) achieves the highest overall success probability, while a network model without BWP (the case with $p_3 = 1$) performs the worst (see Figure 2). Other cases of BWP lie in between these two extreme cases of $p_1 = 1$ and $p_3 = 1$.

**Meta distribution:** Figure 3 plots the per-type SIR meta distribution against the reliability $x$ for different target SIR thresholds $\theta$. The curves in Figure 3 allow one to make precise statements about the fraction of users achieving an SIR of $\theta$ with reliability $x$, which in turn reveal fine-grained performance in wireless networks. Notice that the same trend as the per-type success probability in Figure 1 holds for the SIR meta distribution, *i.e.*, type-1 users outperform type-2 and type-3 users irrespective of the SIR threshold value. In other words, the fraction of type-1 users that achieve a reliability of $x$ for a given SIR threshold $\theta$ is higher than the fractions of type-2 and type-3 users. For instance, the fraction of users achieving an SIR of $-5$ dB with reliability $60\%$ is $0.78$ for type-1 users, $0.74$ for type-2 users, and $0.73$ for type-3 users. We skip the discussion on the overall SIR meta distribution since it follows a similar trend as that of the overall success probability in Figure 2.

**Shannon throughput:** For the Shannon throughput defined in (8), we have some interesting trends. As shown by solid curves in Figure 4, a new trend emerges for the per-type Shannon throughput, where a type-3 user outperforms type-2 and type-1 users. This trend occurs because a higher allocated bandwidth boosts the per-type Shannon throughput, which overcomes the increased interference due to higher bandwidth. Here, note that the users of higher types achieve a higher Shannon throughput at the expense of larger transmit power $kP$ (hence more power consumption), which grows linearly with $k$ (the type of the user).

**Shannon throughput per Joule**: The trend reverses when the per-type Shannon throughput is normalized by the transmit power, *i.e.*, a type-1 user achieves a higher Shannon throughput than type-2 and type-3 users. This reveals the per-type throughput performance per Joule of energy spent, which is useful in understanding the effect of power consumption on the per-type throughput performance—a motivation behind the inclusion of BWP in 5G NR.

Figure 5 shows that the intensity $\lambda$ of the PPP plays a key role in determining the overall Shannon throughput. For small intensity $\lambda$, as shown by solid curves in Figure 5, the network model with no BWP (the model with $p_3 = 1$) achieves a higher overall Shannon throughput than two networks employing BWP with $p_k = 1/3$ and $p_1 = 1$. In contrast, for large $\lambda$, the trend reverses in that the networks with BWP outperform the network with no BWP. The reason behind this behavior is that: for a small $\lambda$, the interference power is relatively small. Hence, a wide bandwidth in the network without BWP boosts the Shannon throughput and overcomes the negative impact of increased interference due to higher bandwidth. Whereas for large $\lambda$, the effect of increased interference dominates and the network with BWP achieves a higher Shannon throughput.

Also, again similar to the per-type Shannon throughput

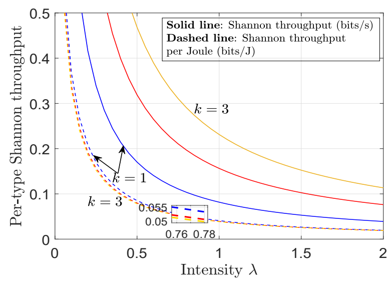


Fig. 4. Per-type Shannon throughput versus intensity $\lambda$. $P = 2$ and $p_k = 1/K = 1/3$. For solid curves: $k = 1, 2, 3$ (from bottom to top). For dashed curves: $k = 1, 2, 3$ (from top to bottom).

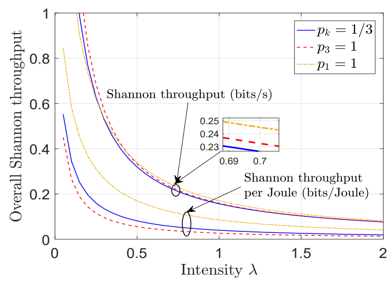


Fig. 5. Overall Shannon throughput versus intensity $\lambda$. $P = 2$.

case, the network without BWP achieves a higher Shannon throughput for small $\lambda$ at the expense of larger transmit power $kP$ (hence more power consumption). Thus, when the Shannon throughput is normalized by the transmit power, the network with the least interference power (the network with $p_1 = 1$ in this case) achieves the highest Shannon throughput.

**Benefits of BWP**: We now briefly discuss the benefits of BWP from these numerical results. Let us start with the user performance viewpoint. It should be clear from Figures 1 and 3 that smaller users (*i.e.*, users of type 1) get a better success probability and a better meta distribution than bigger ones. Note that the improvement is more pronounced for higher SIR thresholds. Figure 4 shows that the Shannon throughput per Joule is also better for smaller users than for bigger ones. We conclude that BWP brings the expected service differentiation and protection of small users, both in terms of success probability and Shannon throughput per Joule. As for bigger users, we see in Figure 4 that they nevertheless get a better Shannon throughput than smaller ones, to the expense of a higher power consumption (proportional to the number of chunks they use). One also gets from first principles that the biggest users get less interference and hence a better Shannon throughput in the scenario with BWP than in the scenario without BWP. Hence, at least for this performance metric, BWP is beneficial to bigger users as well.

Consider now the point of view of operators, namely overall performance, which can be linked to revenue as already mentioned. When comparing the uniform case to the case with $p_3 = 1$ (no BWP case) in Figure 2, we see that the overall success probability is higher in the situation with BWP than in the situation without. Figure 5 actually shows that the same conclusion holds for the overall Shannon throughput per Joule. We conclude that BWP should be beneficial to operators as well. These conclusions are not limited to this special case with three chunks as the ordering of the curves is in fact the same when varying the number of chunks and/or the other model parameters.

### B. Increasing traffic variability may improve performance

Suppose the operator has decided to use BWP and is interested in comparing the overall performance of two networks with different probabilities $p_k$. Consider a first network with uniformly distributed $p_k$, for $K = 3$, $p_k = 1/K = 1/3$. For the second network, also with $K = 3$, assume that $p_3 = 0.7$ and $p_1 = 0.3$. The choice of $p_k$ for the second network is inspired from the estimated proportion of the video traffic for year 2020 [1]. It is expected that approximately 70% of mobile traffic will correspond to videos needing a wide bandwidth. Hence, $p_3 = 0.7$ corresponds to video traffic, while $p_1 = 0.3$ corresponds to non-video traffic due to applications requiring smaller bandwidths. For the second network, the transmit power per chunk $P'$ and the intensity $\lambda'$ are calculated from (18) and (21), respectively, such that both networks have the same mean interference and the same mean signal powers.

Compared to the first network, the second one has a more variable distribution of powers and hence a more variable interference. From Figures 6, 7, and 8, it is clear that the second and more variable traffic network outperforms the first one in terms of all performance metrics: success probability, Shannon throughput, and Shannon throughput per Joule.

For the Shannon throughput case, the trends in both the Shannon throughput and the Shannon throughput per Joule with intensity $\lambda$ are the same (see Figures 7 and 8). This is different from the case without equality of the mean values as shown in Figure 5, where we observed that, for small $\lambda$, the trend in Shannon throughput per Joule is opposite of that in Shannon throughput. Also, there is no a crossover in curves of Shannon throughput with $\lambda$ in the model with balanced means.

## VII. Concluding Remarks and Future Directions

This paper proposes a first analytic model for the prediction of the bandwidth sharing operated by BWP. The proposed model allowed us to show that BWP should benefit to both small and big users. We showed that small users are well protected by BWP in terms of success probability, meta distribution of the SIR, and Shannon throughput per Joule. We also showed that big users achieve a better Shannon throughput than in the situation without BWP. The analysis of overall performance allowed us to show that BWP should also be beneficial to operators. There are several future directions of research. In this work, we focused on D2D networks. A natural extension is to study BWP in cellular settings. It would also be interesting to see how to strategically assign bandwidth chunks to users based on their local environment. Finally, this work is limited to a snapshot analysis of the network. The inclusion of dynamics will certainly be of great interest as well.

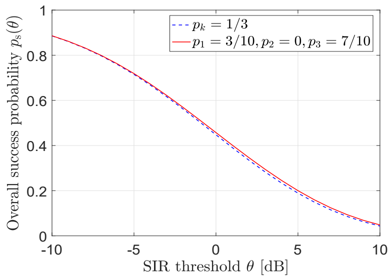


Fig. 6. Overall success probability $p_{\rm s}(\theta)$ versus the SIR threshold $\theta$.

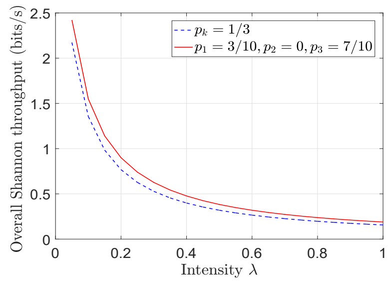


Fig. 7. Overall Shannon throughput versus intensity $\lambda$. $P = 2$.

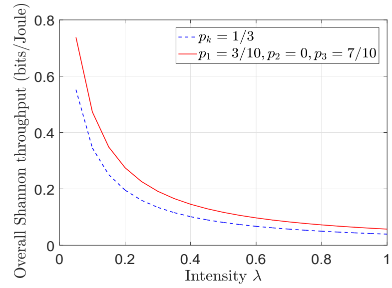


Fig. 8. Overall Shannon throughput per Joule versus intensity $\lambda$. $P = 2$.

## Appendix A
## Proof of Lemma 1

Conditioned on $x_0 \in \Phi_k$, the success probability $p_{\rm s}^{(k)}$ is

$$\begin{aligned} p_{\rm s}^{(k)}(\theta) &= \mathbb{P}(\mathsf{SIR}_o^{(k)} > \theta \mid x_0 \in \Phi_k) \\ &= \mathbb{P}\left(h_{x_0} > \theta \frac{\sum_{i=1}^{K}\sum_{t=0}^{k\wedge i}\sum_{x\in\Phi_{\Phi_{i,t}}\setminus\{x_0\}} t h_x \ell(x)}{k\ell(x_0)}\right) \\ &= \mathbb{E}\left[\exp\left(-\frac{\theta\sum_{i=1}^{K}\sum_{t=0}^{k\wedge i}\sum_{x\in\Phi_{\Phi_{i,t}}\setminus\{x_0\}} t h_x \ell(x)}{k\ell(x_0)}\right)\right]. \end{aligned}$$

Averaging over interfering fading channels, it follows that

$$p_{\rm s}^{(k)}(\theta) = \prod_{i=1}^{K} \underbrace{\prod_{t=0}^{k\wedge i} \mathbb{E}\left[\prod_{x\in\Phi_{i,t}\setminus\{x_0\}} \frac{1}{1+\frac{\theta t\ell(x)}{k\ell(x_0)}}\right]}_{p_{{\rm s}|k}^{(i)}(\theta)}. \tag{22}$$

The probability $p_{\rm s}^{(k,i)}$ can be interpreted as the success probability of the typical receiver due to interference from type-$i$ interferers only conditioned on the typical transmitter being of type $k$. The reason behind this interpretation is that the expression of $p_{\rm s}^{(k,i)}$ in (22) can be obtained by calculating $\mathbb{P}\left(\frac{S}{I_{k,i}} > \theta\right) = \mathbb{P}\left(\mathsf{SIR}_o^{(k,i)} > \theta\right)$, where $S$ is signal power and $I_{k,i}$ given by (2) is the interference power received at the typical receiver only from type-$i$ interferers. Thus, $\mathsf{SIR}_o^{(k,i)}$ is the SIR at the typical receiver when the interference from type-$i$ interferers only is taken into account.

## Appendix B
## Proof of Theorem 1

Continuing from (22), we have

$$p_{\rm s}^{(k,i)}(\theta) = \prod_{t=0}^{k\wedge i} \mathbb{E}\left[\prod_{x\in\Phi_{i,t}\setminus\{x_0\}} \frac{1}{1+\frac{\theta t\ell(x)}{k\ell(x_0)}}\right]. \tag{23}$$

For the power-law path loss model $\ell(r) = r^{-\alpha}$, by the probability generating functional (PGFL) of the PPP, it follows that

$$p_{\rm s}^{(k,i)}(\theta) = \prod_{t=0}^{k\wedge i} \exp\left(-\lambda_{i,t}\int_{\mathbb{R}^2}\left(1-\frac{1}{1+\frac{t\theta R^\alpha \|x\|^{-\alpha}}{k}}\right){\rm d}x\right), \tag{24}$$

where $\lambda_{i,t}$ is the intensity of the point process $\Phi_{i,t}$. Here, $\lambda_{i,t} = \lambda_i p_{k,i}^{(t)}$ since the PPP $\Phi_i$ of interferers of type $i$ is partitioned into $t$ independent PPPs of interferers of type $i$ having $t$ common chunks with the typical transmitter. Solving the integral in (24) and substituting $\lambda_i = \lambda p_i$, we have the desired expression of $p_{\rm s}^{(k,i)}$.

## Appendix C
## Proof of Theorem 2

Conditioning on the typical transmitter $x_0$ being of type $k$, the conditional success probability $P_{\rm s}^{(k)}$ is given as

$$\begin{aligned} P_{\rm s}^{(k)}(\theta) &= \mathbb{P}(\mathsf{SIR}_o^{(k)} > \theta \mid \Phi) \\ &= \mathbb{P}\left(h_{x_0} > \theta\frac{\sum_{x\in\Phi\setminus\{x_0\}} t_x h_x \ell(x)}{k\ell(x_0)} \mid \Phi\right) \\ &= \prod_{x\in\Phi\setminus\{x_0\}} \mathbb{E}\left[\exp\left(-\theta\frac{t_x h_x\ell(x)}{k\ell(x_0)}\right) \mid \Phi\right], \end{aligned}$$

where the expectation is taken over the random channel access scheme of interferers determined by the BWP model and the fading. Recall that, for the BWP model, each interferer can be of type $i$ with probability $p_i$. Then, a type-$i$ interferer can have $0 \le t \le k\wedge i$ chunks common with the typical transmitter with probability $p_{k,i}^{(t)}$. Thus, by averaging over the channel access scheme, it follows that

$$P_{\rm s}^{(k)}(\theta) = \prod_{x\in\Phi\setminus\{x_0\}} \mathbb{E}\left[\sum_{i=1}^{K} p_i \sum_{t=0}^{k\wedge i} p_{k,i}^{(t)} \exp\left(-\theta\frac{t h_x \ell(x)}{k\ell(x_0)}\right) \mid \Phi\right].$$

Now, averaging over the fading on interfering channels yields

$$P_{\rm s}^{(k)}(\theta) = \prod_{x\in\Phi\setminus\{x_0\}} \sum_{i=1}^{K} p_i \sum_{t=0}^{k\wedge i} \frac{p_{k,i}^{(t)}}{1+\theta\frac{t}{k}\frac{\ell(x)}{\ell(x_0)}}.$$

The $b$th ($b \in \mathbb{C}$) moment of $P_{\rm s}^{(k)}$ can be expressed as

$$M_b^{(k)} = \exp\left(-2\pi\lambda\int_0^\infty\left[1-\left(\sum_{i=1}^{K} p_i \sum_{t=0}^{k\wedge i}\frac{p_{k,i}^{(t)}}{1+\theta\frac{t}{k}\frac{\ell(r)}{\ell(x_0)}}\right)^b\right]{\rm d}r\right),$$

when making use of the PGFL of the PPP.

## REFERENCES


[1] (2019). Cisco visual networking index: Global mobile data traffic forecast update, 2017-2022. [Online]. Available: https://www.cisco.com/c/en/us/solutions/collateral/service-provider/visual-networking-index-vni/white-paper-c11-738429.html

[2] White paper (MediaTek). Bandwidth part adaptation: 5G NR user experience and power consumption enhancements. [Online]. Available: https://newsletter.mediatek.com/hubfs/mwc/download/bandwidth-part-adaptation.pdf

[3] 3GPP, "NR: NR and NG-RAN overall description; stage 2," Technical Specification (TS) 38.300, 3rd Generation Partnership Project (3GPP), January 2019. Version 15.4.0.

[4] 3GPP, "NR: Physical channels and modulation," Technical Specification (TS) 38.211, 3rd Generation Partnership Project (3GPP), March 2019. Version 15.5.0.

[5] S. Blake, D. Black, M. Carlson, E. Davies, Z. Wang, and W. Weiss, "An architecture for differentiated services," Internet RFC 2475, December 1998.

[6] K. Thompson, G. J. Miller, and R. Wilder, "Wide-area internet traffic patterns and characteristics," in IEEE Network, vol. 11, no. 6, pp. 10-23, November-December 1997.

[7] K. Papagiannaki, N. Taft, S. Bhattacharyya, P. Thiran, K. Salamatian, and C. Diot, "A pragmatic definition of elephants in internet backbone traffic," in Proceedings of the 2nd ACM SIGCOMM Workshop on Internet measurement (IMW), New York, NY, USA, 175-176.

[8] C. Estan and G. Varghese, "New directions in traffic measurement and accounting: Focusing on the elephants, ignoring the mice," in ACM Transactions on Computer Systems, vol. 21, no. 3, pp. 270-313, August 2003.

[9] N. Brownlee and K. C. Claffy, "Understanding internet traffic streams: Dragonflies and tortoises," in IEEE Communications Magazine, vol. 40, no. 10, pp. 110-117, October 2002.

[10] K.-C. Lan and J. Heidemann, "A measurement study of correlations of internet flow characteristics," in Computer Networks, vol. 50, no. 1, pp. 46-62, 2006.

[11] J. Jeon, "NR wide bandwidth operations," in IEEE Communications Magazine, vol. 56, no. 3, pp. 42-46, March 2018.

[12] A. Yazar and H. Arslan, "Reliability enhancement in multi-numerology-based 5G new radio using INI-aware Scheduling," in EURASIP Journal on Wireless Communications and Networking, 2019. To appear.

[13] S. Stefanatos and A. Alexiou, "Access point density and bandwidth partitioning in ultra dense wireless networks," IEEE Transactions on Communications, vol. 62, pp. 3376-3384, September 2014.

[14] P. Kyasanur, S. Jungmin, C. Chereddi, and N. Vaidya, "Multichannel mesh networks: challenges and protocols," IEEE Wireless Communications, vol. 13, no. 2, pp. 30-36, 2006.

[15] H. Sun, M. Wildemeersch, M. Sheng, and T. Q. S. Quek, "D2D enhanced heterogeneous cellular networks with dynamic TDD," in IEEE Transactions on Wireless Communications, vol. 14, no. 8, pp. 4204-4218, August 2015.

[16] Y. Yuan, P. Bahl, R. Chandra, T. Moscibroda, and Y. Wu, "Allocating dynamic time-spectrum blocks in cognitive radio networks," in Proceedings of the 8th ACM international symposium on Mobile ad hoc networking and computing (MobiHoc), New York, NY, USA, pp. 130-139, 2007.

[17] L. Hamidouche, P. Sens, S. Monnet, and D. Refauvelet, "Toward heterogeneity-aware device-to-device data dissemination over Wi-Fi networks," 2017 IEEE 23rd International Conference on Parallel and Distributed Systems (ICPADS), Shenzhen, pp. 105-112, 2017.

[18] F. Baccelli and B. Błaszczyszyn, Stochastic Geometry and Wireless Networks, Foundations and Trends in Networking. NOW, 2009.

[19] M. Haenggi, J. G. Andrews, F. Baccelli, O. Dousse, and M. Franceschetti, "Stochastic geometry and random graphs for the analysis and design of wireless networks," in IEEE Journal on Selected Areas in Communications, vol. 27, no. 7, pp. 1029-1046, September 2009.

[20] Martin Haenggi, Stochastic geometry for wireless networks, Cambridge University Press, 2013.

[21] J. G. Andrews, F. Baccelli, and R. K. Ganti, "A tractable approach to coverage and rate in cellular networks," in IEEE Transactions on Communications, vol. 59, no. 11, pp. 3122-3134, November 2011.

[22] H. S. Dhillon, R. K. Ganti, F. Baccelli, and J. G. Andrews, "Modeling and analysis of $K$-tier downlink heterogeneous cellular networks," in IEEE Journal on Selected Areas in Communications, vol. 30, no. 3, pp. 550-560, March 2012.

[23] N. Jindal, J. G. Andrews, and S. Weber, "Bandwidth partitioning in decentralized wireless networks, in IEEE Transactions on Wireless Communications, vol. 7, vol. 12, pp. 5408-5419, December 2008.

[24] Y. Zhong, W. Zhang, and M. Haenggi, "Managing interference correlation through random medium access," in IEEE Transactions on Wireless Communications, vol. 13, no. 2, pp. 928-941, February 2014.

[25] S. Lu and Z. Wang, "Spatial transmitter density allocation for frequency-selective wireless ad hoc networks," in IEEE Transactions on Wireless Communications, vol. 18, no. 1, pp. 473-486, January 2019.

[26] M. Haenggi, "The meta distribution of the SIR in Poisson bipolar and cellular Networks," in IEEE Transactions on Wireless Communications, vol. 15, no. 4, pp. 2577-2589, April 2016.

[27] J. Gil-Pelaez, "Note on the inversion theorem," Biometrika, vol. 38, pp. 481-482, December 1951.